ACS Partner Journal

ACCOUNTS of materials research

pubs.acs.org/amrcda

Article

Cooperative Covalent Polymerization of *N*-carboxyanhydrides: from Kinetic Studies to Efficient Synthesis of Polypeptide Materials

Wanying Wang, Hailin Fu, Yao Lin,* Jianjun Cheng,* and Ziyuan Song*

Cite This: *Acc. Mater. Res.* 2023, 4, 604−615

Read Online

ACCESS | Metrics & More | Article Recommendations

CONSPECTUS: Polypeptides, as the synthetic analogues of natural proteins, are an important class of biopolymers that are widely studied and used in various biomedical applications. However, the preparation of polypeptide materials from the polymerization of *N*-carboxyanhydride (NCA) is limited by various side reactions and stringent polymerization conditions. Recently, we report the cooperative covalent polymerization (CCP) of NCA in solvents with low polarity and weak hydrogen-bonding ability (e.g., dichloromethane or chloroform). The polymerization exhibits characteristic two-stage kinetics, which is significantly accelerated compared with conventional polymerization under identical conditions. In this Account, we review our recent studies on the CCP, with the focus on the acceleration mechanism, the kinetic modeling, and the use of fast kinetics for the efficient preparation of polypeptide materials.

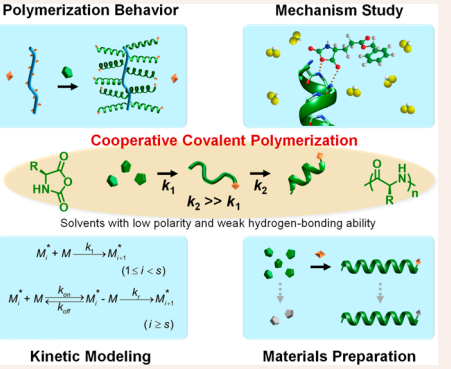

By studying CCP with several initiating systems, we found that the polymerization rate was dependent on the secondary structure as well as the macromolecular architecture of the propagating polypeptides. The molecular interactions between the α-helical, propagating polypeptide and the monomer played an important role in the acceleration, which catalyzed the ring-opening reaction of NCA in an enzyme-mimetic, Michaelis−Menten manner. Additionally, the proximity between initiating sites further accelerated the polymerization, presumably due to the cooperative interactions of macrodipoles between neighboring helices and/or enhanced binding of monomers. A two-stage kinetic model with a reversible monomer adsorption process in the second stage was developed to describe the CCP kinetics, which highlighted the importance of cooperativity, critical chain length, binding constant, $[M]_0$, and $[M]_0/[I]_0$. The kinetic model successfully predicted the polymerization behavior of the CCP and the molecular-weight distribution of resulting polypeptides.

The remarkable rate acceleration of the CCP offers a promising strategy for the efficient synthesis of polypeptide materials, since the fast kinetics outpaces various side reactions during the polymerization process. Chain termination and chain transfer were thus minimized, which facilitated the synthesis of high-molecular-weight polypeptide materials and multiblock copolypeptides. In addition, the accelerated polymerization enabled the synthesis of polypeptides in the presence of an aqueous phase, which was otherwise challenging due to the water-induced degradation of monomers. Taking advantage of the incorporation of the aqueous phase, we reported the preparation of well-defined polypeptides from nonpurified NCAs. We believe the studies of CCP not only improve our understanding of biological catalysis, but also benefit the downstream studies in the polypeptide field by providing versatile polypeptide materials.

1. INTRODUCTION

Polypeptide, consisting of multiple amino acids linked through peptide bonds, is one of the most important classes of polymeric biomaterials.[1−6] As the synthetic analogues of natural proteins, polypeptides exhibit excellent biocompatibility and biodegradability. The versatile design of side chains enables the facile functionalization of polypeptide materials for various biomedical applications.[7−14] Additionally, polypeptides adopt ordered secondary structures such as α-helices and β-sheets.[15,16] The conformation-specific properties and functions not only improve our understanding of natural proteins, but also offer unique materials with promising biomedical performance.

Synthetic polypeptide materials are usually prepared through recombinant technology,[17] solid-phase peptide synthesis,[18] and the ring-opening polymerization (ROP) of amino acid *N*-carboxyanhydrides (NCAs).[19] Among three strategies, the polymerization method is widely used to prepare synthetic polypeptides with high molecular weights (MWs) on a large

Received: March 27, 2023
Revised: May 7, 2023
Published: June 14, 2023

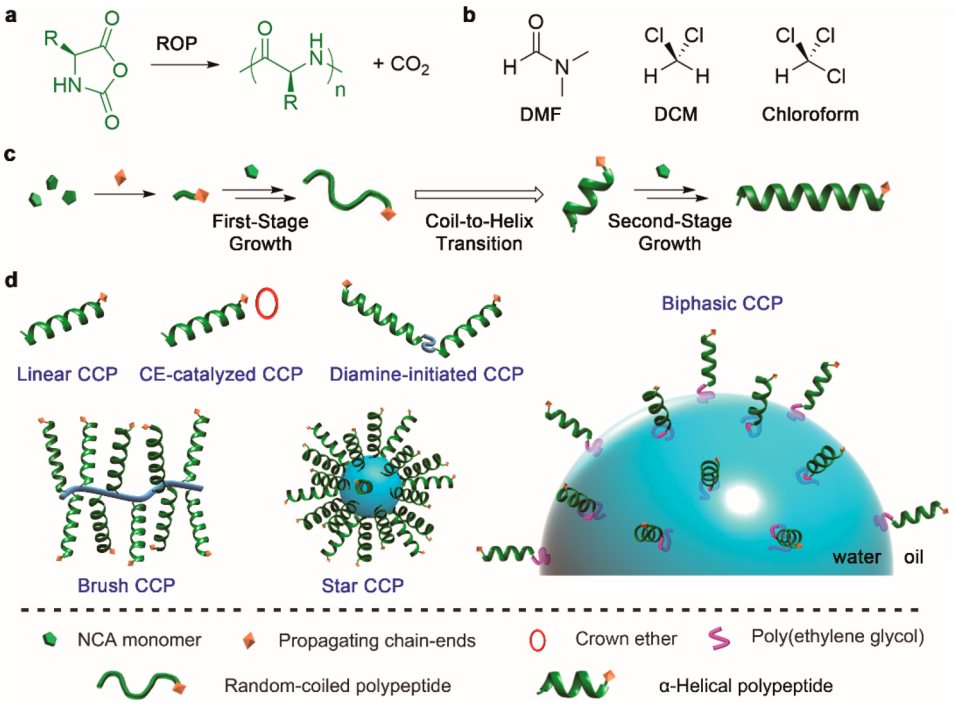

Figure 1. Schematic illustrations of various CCP systems. (a) Synthetic route to polypeptides from NCA. (b) Chemical structure of solvent molecules DMF, DCM, and chloroform. (c) Scheme illustrating the two-stage growth of polypeptides. (d) Schemes showing various CCP systems.

scale (Figure 1a). Since the first synthesis of NCA molecule in 1906,[20] many efforts have been devoted to elucidating the polymerization behaviors of NCAs.[21,22] The development of controlled polymerization techniques in the last three decades enables the preparation of well-defined polypeptides with predictable MWs and narrow dispersity.[23−27] These advances help the design and the synthesis of new polypeptide materials such as the block copolypeptides and brush-like polypeptides, which show interesting assembly behaviors and unique materials properties.

Despite the exciting advances in controlled polymerization strategy, the preparation of polypeptides is limited by various side reactions during the polymerization process.[28,29] For instance, few polymerization systems can generate polypeptides with the degree of polymerization (DP) exceeding 400 in a controlled manner, mainly due to the existence of a trace amount of impurities during monomer synthesis. The moisture-free setup throughout the conventional synthetic procedures, which is inevitable considering the water-induced degradation of the monomers, further limits the preparation of polypeptide materials.

The recent development of accelerated polymerization offers new opportunities for the efficient synthesis of polypeptide materials.[30−49] Through the design of new initiators/catalysts or the changes in polymerization conditions, the polymerization rate is significantly enhanced. The desired polymerization of NCA outpaces various side reactions including the water-induced side reactions,[33,38,43,45] enabling the preparation of well-defined polypeptides even in the presence of an aqueous phase.[38,43,48] Additionally, the accelerated polymerization allows the efficient synthesis of polypeptides with versatile architectures,[31,32,35,42,49] high MWs,[32,34,42,46] and predictable multiblock sequences,[39,45] which is difficult, if not impossible, to obtain with conventional polymerization methods.

NCA polymerization is usually conducted in polar solvents like *N*,*N*-dimethylformamide (DMF) to fully dissolve the monomers and resulting polypeptides (Figure 1b). We recently discovered that the polymerization of NCA in solvents with low polarity and weak hydrogen-bonding (H-bonding) ability, such as dichloromethane (DCM) and chloroform (Figure 1b), exhibited two-stage polymerization kinetics resembling the cooperative supramolecular polymerization (Figure 1c).[32] The polymerization was named *cooperative covalent polymerization* (CCP). Compared to the conventional polymerization in DMF, CCP with a fast, self-catalyzed second stage showed an enhanced overall polymerization rate under identical conditions.[40] Therefore, the studies on CCP not only shed light on the understanding of biomimetic catalysis, but also offer a facile strategy to efficiently synthesize polypeptide materials. Various CCP systems were developed, including the linear CCP, the crown ether (CE)-catalyzed CCP, the multi-amine-initiated CCPs (from diamine, multi-amine, or dendritic initiators), and the biphasic CCP from assembled macroinitiators (Figure 1d). The features of various CCP systems were summarized in Table 1.

In this Account, we first review our current understanding of the CCP, including the solvent dependence, the key structural factors, and the MW control. The acceleration mechanism and the kinetic modeling are highlighted, which may help the future design of accelerated systems. The use of the accelerated effect of the CCP in materials synthesis is then summarized, with an emphasis on the simplification of polymerization procedures by outpacing various side reactions. Finally, we discuss the unsolved challenges and the future directions of the CCP. With the summary and in-depth discussion on the solvent-dependent, accelerated polymerization of NCA and its applications in polypeptide synthesis, we believe this Account serves as a nice complement to the existing review articles on NCA/polypeptides, which focused on chemistry,[10,28] materials

https://doi.org/10.1021/accountsmr.3c00046
Acc. Mater. Res. 2023, 4, 604−615

Table 1. Summary of Various CCP Systems

entry	CCP system	t (min)[a]	σ^{-1}[b]	highlighted features
1	linear	350	3−23	polymerization dependent on $[M]_0$
2	CE	18	ND	CE catalysis regardless of initiator structure
3	diamine	40	8−740	tunable rates by linker length
4	brush	35	44−37 000	tunable rates by brush density
5	star	5	ND	fast rate for all generations of PAMAM core
6	biphasic	16	−[c]	polymerization of nonpurified NCA

[a]Polymerization time reaching 95% monomer conversion with a synthesis of 100-mer polypeptides. $[M]_0$ = 50 mM except for the linear (200 mM) and diamine (100 mM) CCP. [b]Apparent cooperativity ratio defined as the ratio between k_2 and k_1. Obtained from the CCP kinetic model without the Michaelis−Menten factors. ND = not determined. [c]Polymerization without a first stage due to the use of α-helical macroinitiators.

design,[2−6,8,9] self-assembly,[7] secondary structure,[15,16] and biomedical application.[1,2,4−6,8,11−14]

2. POLYMERIZATION BEHAVIORS

2.1. Solvent Dependence

Unlike conventional NCA polymerization that is conducted in polar solvents, CCP requires solvents with low polarity and weak H-bonding ability. A typical CCP profile in DCM (ε = 9.08), as shown in Figure 2a, revealed two-stage, sigmoidal kinetics.[40] In contrast, the conventional polymerization in polar DMF (ε = 36.7) was one-stage, with a much slower rate under identical conditions (Figure 2a). When CCP was conducted in various chlorinated solvents, the polymerization rate followed the order of the solvent polarity, with faster polymerization in solvents with a lower dielectric constant (Figure 2b).[32] Besides the solvent polarity, the H-bonding ability of the solvent molecule was also critical. The two-stage kinetics was not observed in less polar tetrahydrofuran (THF, ε = 7.58),[37,46] which was attributed to its strong H-bonding acceptor ability (H-bonding acceptor basicity β = 0.523).

Moreover, the CCP kinetics exhibited a strong dependence on the initial concentration of monomer, $[M]_0$ (Figure 2c), enabling us to further shorten the polymerization time.[40] At a monomer concentration close to its solubility in DCM (i.e., $[M]_0$ = 0.4 M for γ-benzyl-L-glutamate NCA, BLG-NCA), the CCP at a monomer-to-initiator ratio ($[M]_0/[I]_0$) of 100 in the presence of 18-crown-6 (18-C-6), a CE catalyst, was completed in 2 min,[46] which was comparable to the polymerization with an activated monomer mechanism (AMM) (e.g., initiated by triethylamine).

2.2. Structural Factors Contributing to the Acceleration

The two-stage kinetics stems from the coil-to-helix transition of propagating polypeptides at the DP ∼ 8−12, with faster polymerization at the α-helical stage.[32] For instance, the brush CCP reached ∼10% conversion at 16 min with a random-coiled structure, and was then remarkably accelerated after the α-helical conformation became stable, with >90% monomers consumed in 10 min.[32] The in situ Fourier transform infrared spectroscopy (FTIR) and circular dichroism (CD) confirmed the transition of the secondary structure during the polymerization (Figure 3a).[32]

The helix-associated acceleration was further validated by the polymerization from a pre-existing α-helical poly(γ-benzyl-L-glutamate) (PBLG) macroinitiator, which exhibited one-stage, fast polymerization kinetics.[32] Additionally, the polymerization of racemic DL monomers, devoid of α-helical propagating chains, was much slower compared with that of enantiopure L or D monomers (Figure 3b).[32,37,42,46] On the other hand, NCAs with other side chains exhibited similar two-stage polymerization behaviors.[32,38,40,46]

Besides the control over the secondary structure, the tuning of the spatial organization of initiating sites provides an alternative strategy to manipulate the polymerization rate (Figure 3c).[32] For example, the polymerization from a dense, brush-like macroinitiator was rapid even at a low $[M]_0$ (i.e., 0.05 M), reaching >98% monomer conversion in 1 h. In sharp contrast, the polypeptide growth from a small-molecular initiator proceeded slowly, with ∼30% conversion observed after 24 h under the same conditions (Figure 3d).[32] By tuning the density of amino groups on the macroinitiators, we were able to tune the polymerization rate, with a faster polymerization at a higher density of initiating sites.[32,37,42] In addition, the connection of propagating polypeptide chains was not limited to covalent linkages. The polymerization from methoxy poly(ethylene glycol)-*block*-PBLG amine (PEG-PBLG), an amphiphilic macroinitiator, showed much faster polymerization kinetics than that from a PBLG initiator in a water/DCM biphasic system (Figure 3e).[38] The amphiphilic feature

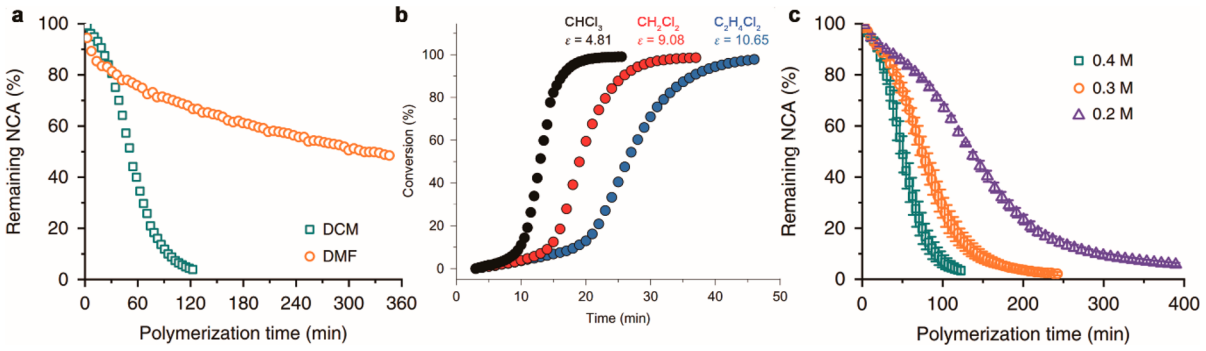

Figure 2. Solvent-dependent polymerization behaviors of NCA. (a) Conversion of NCA in linear polymerizations in DCM and DMF. Reproduced with permission from ref 40. Copyright 2019 Nature Publishing Group. (b) Conversion of NCA in brush CCPs in various chlorinated solvents. Reproduced with permission from ref 32. Copyright 2017 Nature Publishing Group. (c) Conversion of NCA in linear CCPs at various $[M]_0$. Reproduced with permission from ref 40. Copyright 2019 Nature Publishing Group.

https://doi.org/10.1021/accountsmr.3c00046
Acc. Mater. Res. 2023, 4, 604−615

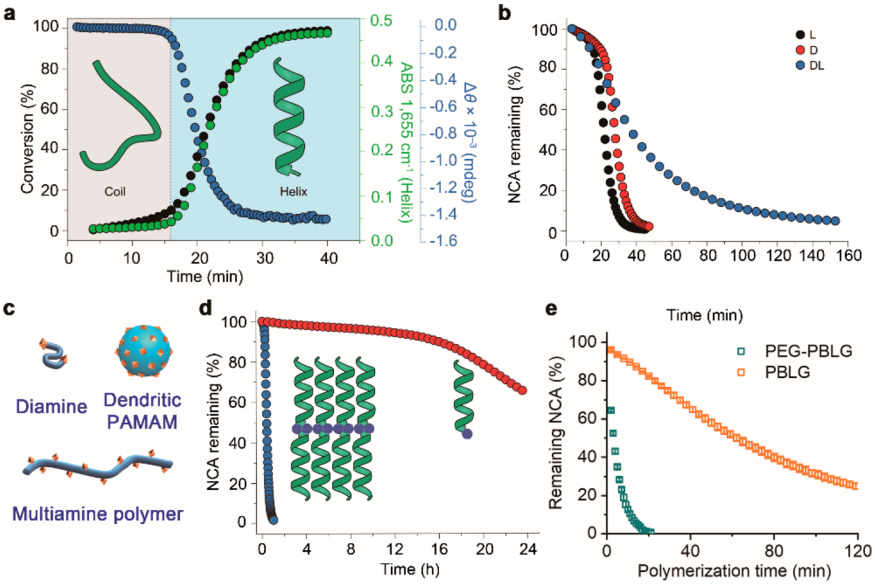

Figure 3. Molecular-structure-dependent rate acceleration in the CCP. (a) Formation of α-helix as evidenced by the increase in FTIR absorbance at 1655 cm^{-1} and CD ellipticity at 227.9 nm. The change in polymerization rate coincided with the transition of secondary structures. (b) Conversion of NCA monomers with different chirality, including enantiopure L/D monomers and racemic monomers. (c) Schematic illustration of multi-amine CCP (macro)initiators. The initiating sites are presented as orange diamonds. (d) Conversion of NCA in brush and linear CCPs. Reproduced with permission from ref 32. Copyright 2017 Nature Publishing Group. (e) Conversion of NCA in biphasic CCPs initiated by oil-dispersed PBLG and interfacially assembled PEG−PBLG macroinitiators. Reproduced with permission from ref 38. Copyright 2019 National Academy of Sciences.

Table 2. Characterization of Obtained Polypeptides in Various CCP Systems[a]

entry	initiator[b]	system	$[M]_0$ (mM)	$[M]_0/[I]_0$	t (min)[c]	M_n (M_n*)[d] (kDa)[e]	$Đ$[e]	IE (%)[f]
1	Hex-NH_2	linear	200	100	180	23.9 (22.0)	1.09	
2	PNB	brush	50	100	32	88.8 (21.8)	1.03	24.5%
3	Hex-NH_2	CE	50	100	18	136.0 (22.0)	1.21	16.2%
4	Hex-NH_2	CE	200	100	5	107.0 (22.0)	1.28	20.6%
5	Hex-NH_2	CE	400	100	2	88.7 (22.0)	1.33	24.8%
6	PNB	brush	50	50	30	65.5 (11.0)	1.03	16.8%
7	PNB	brush	50	200	50	134.0 (43.4)	1.03	32.4%
8	Hex-NH_2	CE	25	50	12	76.4 (11.1)	1.24	14.5%
9	PBLG	CE	100	50	14	19.7 (18.3)	1.06	

[a]All polymerizations were conducted in DCM with BLG-NCA as monomers. [b]Hex-NH_2 = *n*-hexylamine, PNB = polynorbonene with pendant trimethylsilyl amino groups, PBLG = *n*-hexyl poly(γ-benzyl-L-glutamate) amine. [c]Polymerization time reaching 95% monomer conversion. [d]Obtained MW (expected MW*). [e]Determined by GPC. [f]Apparent initiation efficiency = expected MW/obtained MW.

of PEG-PBLG led to its assembly at the water/DCM interface, which brought the initiating sites in close proximity, resulting in an accelerated polymerization.

2.3. Control over Molecular Weights

The two-stage kinetics with a faster second stage resulted in a bimodal molecular-weight distribution (MWD) of the resulting polypeptides, as the propagating chains entering the second stage outgrew those staying in the first stage. Such bimodal MWD was not obvious in the linear CCP due to smaller cooperativity,[40] but became pronounced in some ultrafast CCP systems, including the brush CCP and the CE-catalyzed CCP (Table 2, entries 1−3).[32,46] The apparent initiation efficiency (IE), defined as the ratio of expected MW to the obtained MW, was calculated to be 15−46% in those two accelerated CCP systems, suggesting that a considerable fraction of initiating sites failed to enter the second stage.[32,46]

While the increase in either $[M]_0$ or $[M]_0/[I]_0$ lowered the oligomeric fraction of CCP (i.e., polypeptide chains with DP < 10), the obtained MW was still much larger than the expected MW (Table 2, entries 4−7).[32,46] To achieve better control over MW, we prepared the α-helical macroinitiator to skip the slower first stage, which ensured all propagating chains grew simultaneously at a similar rate.[38,46] The use of a helical PBLG macroinitiator significantly improved the MW control, where the obtained MW agreed well with the expected value even in some fast CCP systems (Table 2, entries 8 and 9).

3. POLYMERIZATION MECHANISM

The in-depth analysis of the polymerization behavior offered valuable information to elucidate the CCP mechanism. Because both the propagating polypeptides and the NCA monomer were polar, we reasoned that the critical solvent requirement of the CCP might originate from the interactions between the two reactants. While the polar DMF solvent molecules were disruptive, DCM ensured efficient molecular bindings between the propagating chains and the monomer, leading to accelerated ring-opening reactions. To validate our hypothesis, the saturation-transfer difference (STD) NMR was

https://doi.org/10.1021/accountsmr.3c00046
Acc. Mater. Res. 2023, 4, 604−615

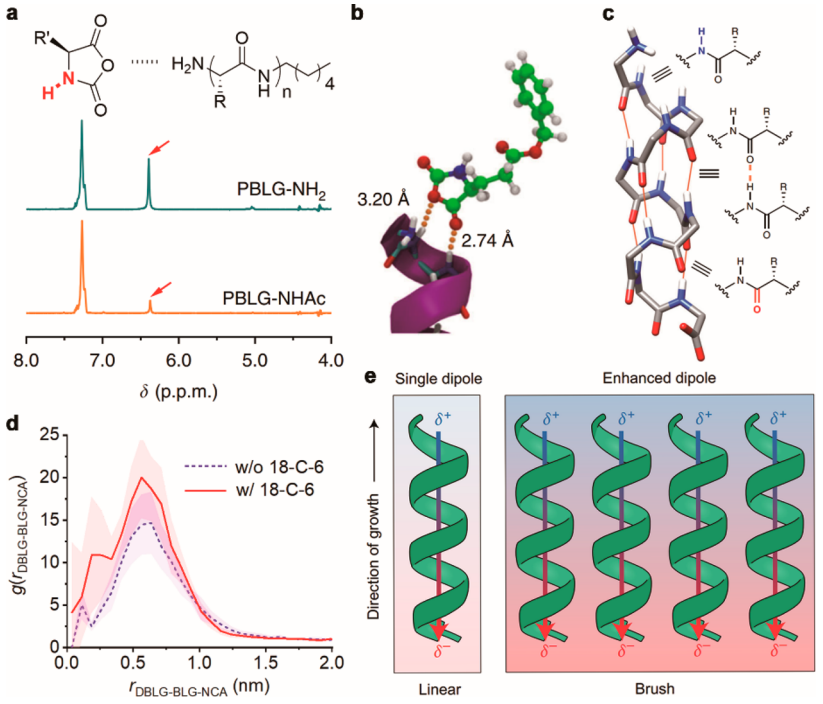

Figure 4. Elucidation of CCP mechanisms. (a) STD NMR spectra of NCA in the presence of a polypeptide chain with an exposed (PBLG-NH_2) or a capped (PBLG-NHAc) N-terminus. (b) Close-up of molecular dynamics simulation trajectories illustrating the binding interactions. The polypeptide backbone was represented as a purple ribbon. (c) Illustration of the distribution of polar groups in an α-helical polypeptide chain. Reproduced with permission from ref 40. Copyright 2019 Nature Publishing Group. (d) Radial distribution functions in the center-of-geometry distance between an NCA monomer and a model propagating molecule (DBLG) in the presence and absence of 18-C-6. Reproduced with permission from ref 46. Copyright 2021 Nature Publishing Group. (e) Illustration showing the array of aligned α-helices with an enhanced dipole in the brush CCP compared to the linear CCP. Reproduced with permission from ref 32. Copyright 2017 Nature Publishing Group.

employed to probe the binding interactions, which showed that the ring N−H protons of the NCA monomer were spatially correlated with the polypeptides (Figure 4a).[40] Upon the capping of the N-terminus, a significant decrease in STD signals was observed, suggesting that the terminal amino group served as the binding site. Additionally, the binding interactions were directly visualized with molecular dynamics simulations, which agreed well with the STD NMR results (Figure 4b).[40]

The confirmation of polypeptide−monomer binding helped us to elucidate the mechanism of helix-associated rate acceleration. With intrahelical hydrogen bonds, the polar groups in an α-helix were only positioned at the two termini (Figure 4c).[40] Hence, the molecular interactions of the monomer with half of the binding sites led to the ring-opening reaction (the effective binding at the N-terminus was even higher considering the bulky *n*-hexyl group at the C-terminus). In contrast, the backbone peptide bonds in a random-coiled polypeptide interacted nonspecifically with the monomers and interfered with the effective N-terminus binding.

With the clarification of the helix-catalyzed polypeptide growth, the catalytic mechanism of CE became obvious. The formation of the CE/amine/NCA tertiary complex was verified by both experimental and simulation-based methods,[46] which brought the amine and NCA in closer proximity than that with an amine/NCA binary complex (Figure 4d), leading to the accelerated polymerization rate.

Meanwhile, the mechanism of proximity-induced rate acceleration is still under investigation, mainly due to the complexity of the system. Compared with the linear CCP, the polymerization from multi-amine initiators resulted in an array of α-helices after entering the second stage (Figure 4e). The local enrichment of monomers and chain-ends might contribute to the enhancement of the apparent binding constants in both stages.[32,50] Fortunately, the accelerated polymerization from diamine and poly(amidoamine) (PAMAM) initiators suggested that the close-proximity effect could be simplified to a system containing only 2−4 initiating sites, which might facilitate the mechanism studies.[37,42]

4. POLYMERIZATION KINETICS

Although rare in synthetic polymer chemistry, the sigmoid-shaped kinetic curve containing a slow "nucleation" stage and a fast propagation stage is reminiscent of the cooperative polymerization behavior in the supramolecular system.[51−53] Therefore, a two-stage nucleation-controlled model was established from the cooperative polymerization theory originally developed for the supramolecular systems.[32,54] This simple model (CCP model) was capable of fitting the two-stage kinetic behaviors and revealing the different levels of cooperativity in various CCP systems.[32,37,38,40] Later, to account for the key effect of monomer adsorption at the growing site in the accelerated stage, a Michaelis−Menten-type equation was incorporated in the rate equations to establish a more sophisticated kinetic model (MM-CCP model).[40,50] This new model not only accounted for the dependence of kinetic profiles on the monomer concentrations and the remarkable effect of macromolecular architectures on the cooperativity, but also correctly predicted the averaged MWs and MWDs of resulting polymers. Besides, it may be used as a generalized form for more complicated polymerization mechanisms, for example, reactions with multiple intermediates or many

https://doi.org/10.1021/accountsmr.3c00046
Acc. Mater. Res. 2023, 4, 604−615

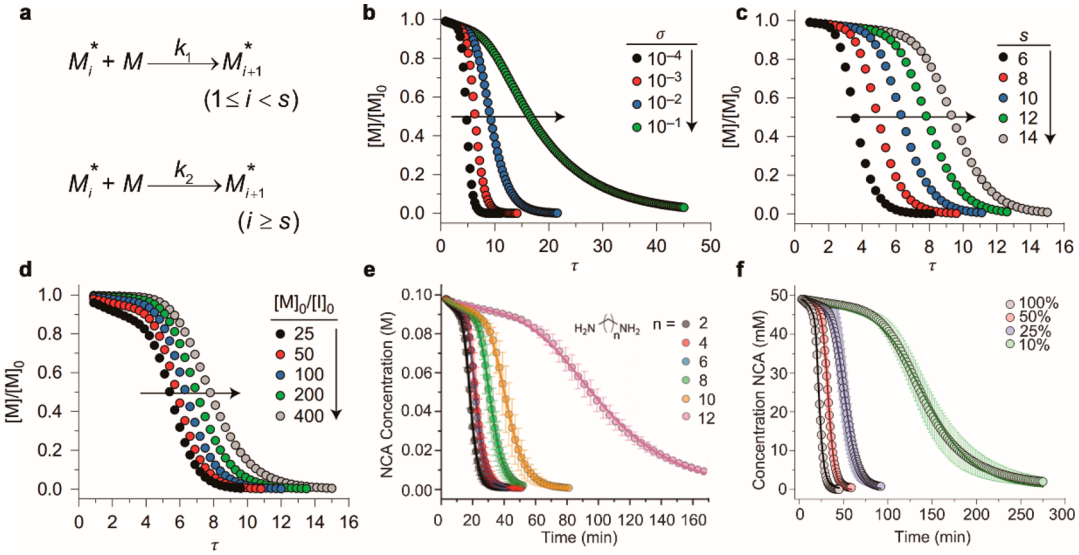

Figure 5. Two-stage CCP kinetic model. (a) Scheme of the two-stage CCP kinetic model. M_i* represents the propagating chains with a DP of *i*. *M* is the monomer. *s* is the critical DP for the coil-to-helix transition. k_1 and k_2 are the propagation rate constants. (b–d) Simulation of the two-stage CCP kinetics as a function of σ, *s*, and $[M]_0/[I]_0$. Reproduced with permission from ref 32. Copyright 2017 Nature Publishing Group. (e) Fittings of the monomer depletion kinetics for diamine-initiated CCPs. Reproduced with permission from ref 37. Copyright 2019 American Chemical Society. (f) Fittings of the monomer depletion kinetics for brush CCPs with different densities of initiating sites. Reproduced with permission from ref 32. Copyright 2017 Nature Publishing Group.

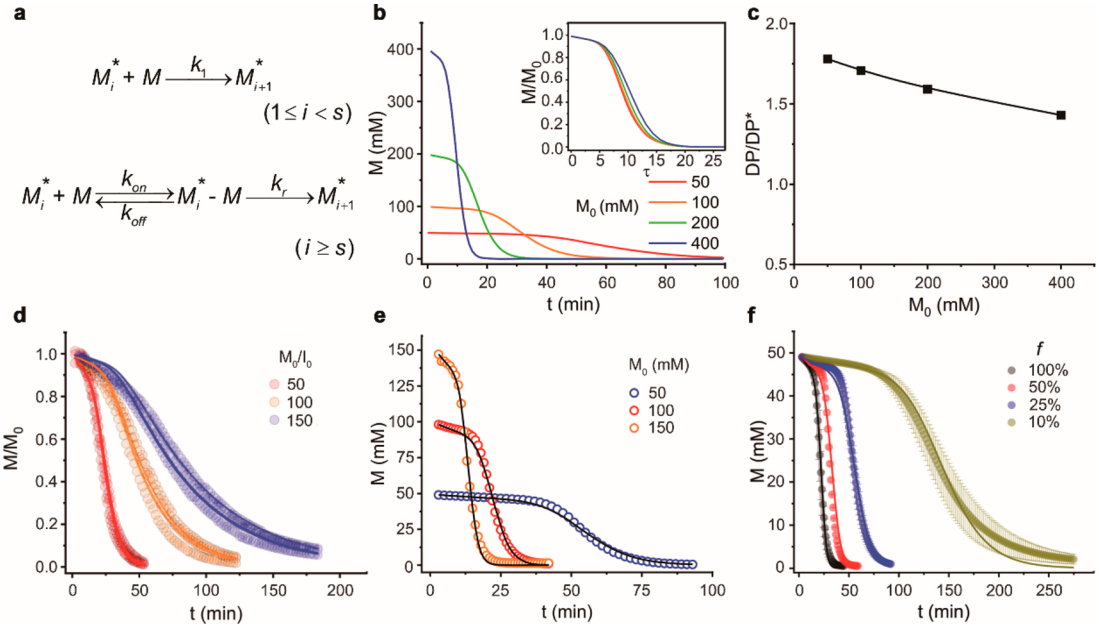

Figure 6. Two-stage, Michaelis–Menten-type CCP kinetic model. (a) Scheme of the kinetic model. In the second stage, the propagating chain M_i* first forms the intermediate $M_i^* - M$ with the rate constants of k_{on} and k_{off}, before the generation of M_{i+1}* with a rate constant of k_r. (b,c) Simulations of the kinetic curves (b), the dimensionless form (the inset of b), and the corresponding averaged DP to DP* ratio as a function of $[M]_0$ (c). (d–f) Fittings of the kinetic curves with the two-stage, Michaelis–Menten-type CCP kinetic model for linear CCPs with different $[M]_0/[I]_0$ (d), diamine-initiated CCPs with different $[M]_0$ (e), and brush CCPs with different densities of initiating sites (f). Reproduced with permission from ref 50. Copyright 2022 American Chemical Society.

competing pathways.[50] The key feature lies in the interplay between noncovalent and covalent interactions and the catalytic nature of the binding event in this unique type of autoaccelerated, helical polymerization.

4.1. Two-Stage Kinetic Model

The model contains two chain-growth stages with the rate constants as k_1 and k_2, respectively (Figure 5a).[32,50] The dimensionless ratio $\sigma = k_1/k_2$ represents the kinetic cooperativity: a number between 0 and 1; and the smaller σ, the greater cooperativity. A growing chain enters the second stage when it reaches a critical chain length, *s*, which represents the minimal chain length for the coil-to-helix transition. The value of *s* is usually in the range of 8–12 for the systems that have been examined so far. The initiation step was often so fast that the model assumes all initiators were consumed at the starting time point.

https://doi.org/10.1021/accountsmr.3c00046
Acc. Mater. Res. 2023, 4, 604–615

Transformation of the kinetic equations into the dimensionless form clearly showed that the kinetics is controlled by only three factors: σ, s, and $[M]_0/[I]_0$.[32] Simulations with the numerical method demonstrated experiment-resembling sigmoidal curves, whose sharpness of the transition, length of the first stage, and shape were governed by σ, s, and $[M]_0/[I]_0$, respectively (Figure 5b–d).[32] Applying the simple two-stage model to the fitting of the monomer depletion kinetics resulted in a good agreement with the experimental results (Figure 5e,f).[32,37] In several CCP systems that had different chain proximity, the model showed that the strength of cooperativity was highly correlated with the interchain distance or chain density.[32,37,38,40] However, the model tends to be less accurate in the prediction of MWs and MWDs for small σ, and cannot explain the dependence of polymerization on the monomer concentration.[50] To solve the problem, a more sophisticated model was developed afterward by considering the binding equilibrium between the monomer and the active chain-ends explicitly.

4.2. Two-Stage, Michaelis–Menten-Type Kinetic Model

With experimental evidence of the reversible binding of NCA to the N-terminus, we incorporated a Michaelis–Menten-type mechanism in the second growth stage (Figure 6a).[40,50] In this model, the growing helical chain (M_i*, $i \geq s$) would first form into an intermediate (M_i* − M) by reversible adsorption and desorption of monomers with the rate constants of k_{on} and k_{off}, respectively. The intermediate then reacts to become a longer growing chain (M_{i+1}*) with a rate constant of k_r. Assuming that k_{off} is much greater than k_r and the intermediate is in a quasi-steady state, the monomer consumption rate (r) for the second stage can be described by the Michaelis–Menten-type equation:

$$r = \frac{k_r[M][P]}{K_D + [M]}$$

where $[M]$ is the monomer concentration, $[P]$ is the concentration of growing helical chains, and K_D (equals to k_{off}/k_{on}) is the dissociation equilibrium constant.

The rate equations of this new model show that the kinetics are not only controlled by σ, s, and $[M]_0/[I]_0$ but also functions of $[M]_0$ and K_D. For example, in the numerical simulations, the monomer-concentration dependence is evidenced in both the dimensionless kinetic curves and the MWD (Figure 6b,c).[50] The binding constant (K_D^{-1}) has to do with the magnitude of this effect.[50] Compared to the simpler two-stage model, the new model predicted much narrower MWD and smaller MW from the same apparent cooperativity.[50] This was attributed to the buffering effect of the reversible adsorption of monomers in the second stage. Applying this new model to the kinetic analysis of systems with different σ, $[M]_0$, and $[M]_0/[I]_0$, it correctly accounted for both the monomer depletion kinetic curves and the averaged MWs (Figure 6d–f).[40,50] While k_r was shown to be almost constant across systems with different levels of cooperativity, the binding constant was found to be correlated with the effective molarity of the chain-ends. It suggests that the local enrichment of growing chains could lead to enhanced monomer adsorption and eventually contribute to the acceleration of the CCP and the enhanced apparent cooperativity. Altogether, the two levels of cooperativity correlated with the α-helical structure and the macromolecular structures could both be attributed to the binding event.

Besides, the Michaelis–Menten-type CCP model was further demonstrated to be a good approximation for polymerization with more complicated mechanisms.[50] The parameters K_D and k_r no longer represent a single chemical or physical event, but are a combination of multiple rate constants and equilibrium constants. This model is envisioned to be generally applicable in predicting the kinetic behaviors and MWDs of other types of CCPs, which combine covalent and noncovalent interactions in the polymerization process.

5. EFFICIENT SYNTHESIS OF POLYPEPTIDE MATERIALS

Despite the promising properties of polypeptides, various side reactions occur during the ROP of NCA, which greatly limits the preparation and downstream applications of polypeptide materials (Figure 7a). On one hand, the ring anhydride group

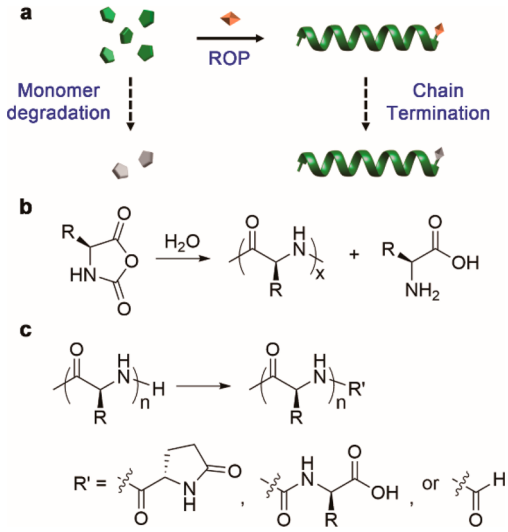

Figure 7. Side reactions during the ROP of NCA. (a) Scheme illustrating side reactions that lead to the monomer degradation or chain termination. (b) Chemical equation showing the degradation of NCA in the presence of water. (c) Chemical equation revealing the degradation of propagating chain-end.

of the NCA monomer is sensitive to many nucleophiles including water.[28] Therefore, anhydrous setups are inevitable during the synthesis, polymerization, and storage of NCA monomer, which otherwise degrades into an amino acid or an oligopeptide in the presence of ambient moisture (Figure 7b). On the other hand, the terminal amino group of the propagating polypeptides may react with the polypeptide side chains or solvent molecules, leading to chain termination or chain transfer (Figure 7c).[27,55] As a result, special initiators/catalysts or stringent polymerization conditions are required to minimize these side reactions.[28]

Unlike conventional strategies that suppress the side reactions through the restriction of polymerization conditions, the accelerated polymerization design outpaces various side reactions by increasing the rate of the main reaction. Controlled polymerization was achieved with conventional primary amines as initiators under ambient conditions. This new strategy thus significantly lowers the cost of polypeptide preparation by circumventing the stringent polymerization setups and the design of special reagents. For instance, CE-catalyzed CCP at $[M]_0/[I]_0$ = 1000 completed within 6 h,

https://doi.org/10.1021/accountsmr.3c00046
Acc. Mater. Res. 2023, 4, 604–615

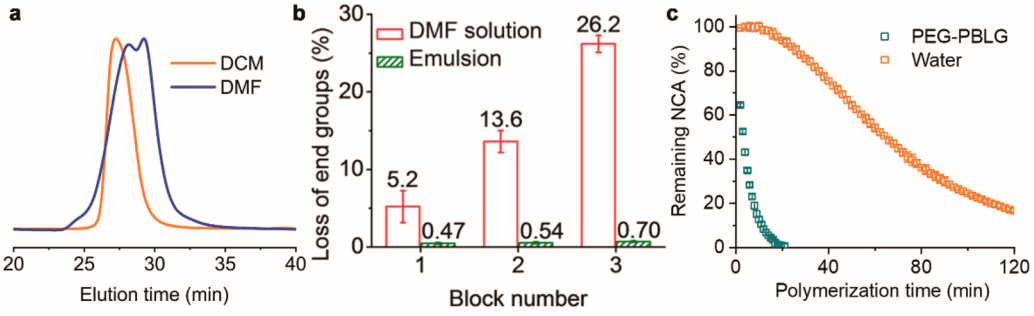

Figure 8. Minimized side reactions in the CCP. (a) Normalized GPC traces of the obtained polypeptide from CE-catalyzed polymerizations in DCM and DMF. $[M]_0/[I]_0 = 1000$. Reproduced with permission from ref 46. Copyright 2021 Nature Publishing Group. (b) Characterization of end-group fidelity during the synthesis of triblock copolypeptides in a biphasic CCP and a DMF solution. Reproduced with permission from ref 39. Copyright 2019 American Chemical Society. (c) Conversion of NCA in biphasic CCPs initiated by PEG−PBLG macroinitiator and degraded by water. Reproduced with permission from ref 38. Copyright 2019 National Academy of Sciences.

which minimized the chain-transfer side reaction as revealed in the conventional DMF polymerization under identical conditions (Figure 8a).[46] The fast CCP also benefited the preparation of multiblock copolypeptides, which requires a high end-group fidelity throughout the polymerization process.[39] Conventional synthesis of triblock copolypeptides in DMF took more than 3 days to finish, with a loss of 26.2% terminal amines. In sharp contrast, the chain termination of biphasic CCP was significantly suppressed to <1% due to rapid kinetics (Figure 8b).

With sufficient rate acceleration, CCP outpaced the water-induced degradation of monomer in the presence of an aqueous phase.[38] Specifically, the biphasic CCP rapidly consumed all NCA monomers within 20 min. Meanwhile, water-induced degradation of NCA was negligible in the first 20 min under identical conditions (Figure 8c). Kinetic modeling results further supported the minimal loss of monomers, which indicated that >99.9% of NCA was polymerized rather than degraded.[38]

5.1. Efficient Synthesis of High-Molecular-Weight Polypeptides

Due to the chain termination and chain transfer, it is difficult to obtain large synthetic polypeptides (DP > 400) in a controlled manner with conventional polymerization methods. The previous synthesis relied on the polymerizations with an AMM to prepare high-MW polypeptides, however, with poor control over MWs and dispersity.[28] In contrast, the fast kinetics and the minimized chain terminations/transfers facilitated the preparation of high-MW polypeptides. CE-catalyzed CCP yielded a series of linear polypeptides with predictable MWs and narrow dispersity (Figure 9a).[46] The synthesis of the largest linear PBLG, with a MW of 2.3×10^5 Da, was completed within 6 h (Table 3).

With several initiating sites confined in one molecule, the polymerization from multi-amine macroinitiators exhibited fast kinetics, generating versatile polypeptide materials with branched architectures (Figure 9b,c).[32,42] It has to be noted that the well-defined polypeptides with narrow MWD were observed in CCP solvents but not conventional solvents, highlighting the important role of rate acceleration.[32,42] The multi-amine CCP system produced some of the largest synthetic polypeptides in a controlled manner. The highest MW tested for the brush- and star-like polypeptides were determined to be 43 and 85 MDa, respectively (Table 3), both much higher than the MW of the largest protein reported to date (i.e., titin, ~4 MDa).[32,42]

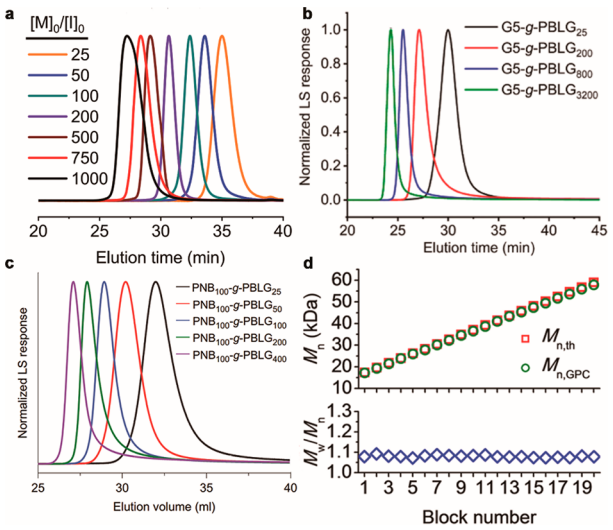

Figure 9. Efficient synthesis of various polypeptide materials. (a−c) Normalized GPC traces of obtained polypeptides from CE-catalyzed CCPs (a), star CCPs (b), and brush CCPs (c) at different $[M]_0/[I]_0$. Reproduced with permission from refs 46, 42, and 32. Copyright 2021 Nature Publishing Group, 2020 American Chemical Society, and 2017 Nature Publishing Group, respectively. (d) Plot of the theoretical ($M_{n,th}$) and the experimental ($M_{n,GPC}$) MWs and the dispersity of each intermediate copolypeptides during a 20-block copolypeptide synthesis in a biphasic CCP. Reproduced with permission from ref 39. Copyright 2019 American Chemical Society.

Table 3. Preparation of High-MW Polypeptide Materials

polymer	system	$[M]_0/[I]_0$	M_n (M_n*) (MDa)[a]	$Đ$[b]
$PBLG_{1030}$	CE	1000	0.23 (0.226)	1.09
PNB_{200}-*g*-$PBLG_{400}$	brush	400	16.6 (17.3)	1.03
PNB_{400}-*g*-$PBLG_{400}$	brush	400	43.3 (36.4)	1.04
PAMAM(G3)-*g*-$PBLG_{3200}$	star	3200	22.6 (22.4)	1.03
PAMAM(G5)-*g*-$PBLG_{3200}$	star	3200	85.1 (89.6)	1.01

[a]Obtained MW (expected MW*). [b]Determined by GPC.

5.2. Synthesis of Versatile Multiblock Copolypeptides

The high end-group fidelity throughout the polymerization process makes the CCP a promising system to prepare multiblock copolypeptides.[39] By sequential addition of NCA monomers into a biphasic CCP system, well-defined multi-

https://doi.org/10.1021/accountsmr.3c00046
Acc. Mater. Res. 2023, 4, 604−615

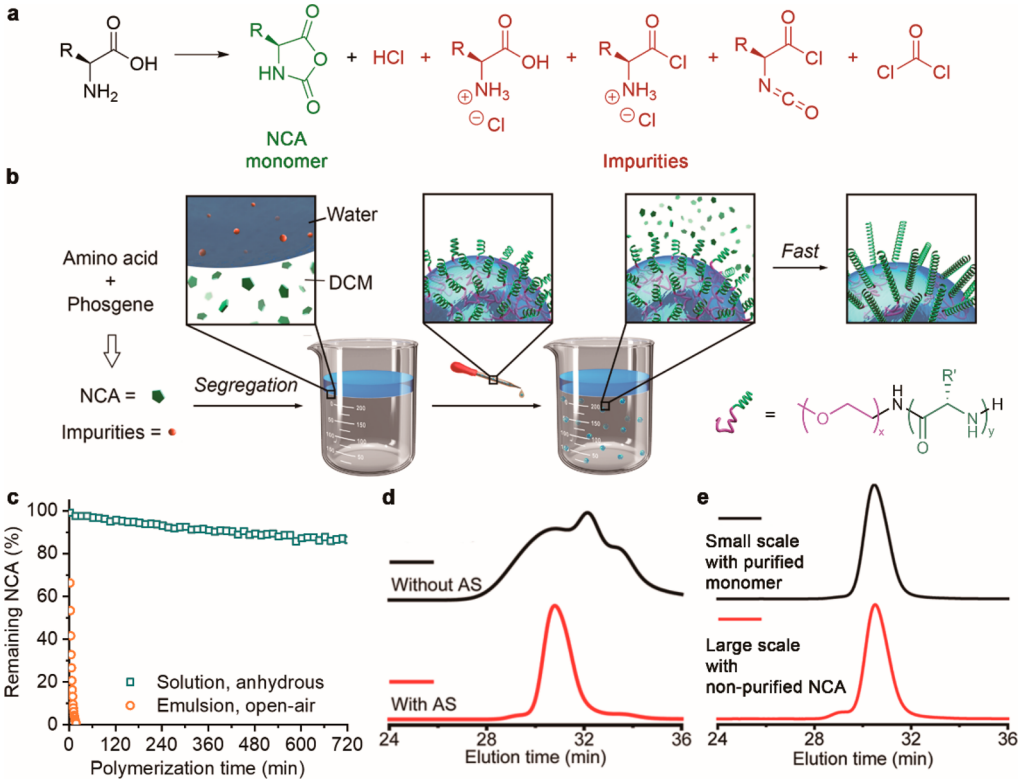

Figure 10. Polymerization of nonpurified monomers. (a) Chemical structures of impurities generated during the NCA synthesis. (b) Scheme illustrating the process of SIMPLE polymerization based on the biphasic CCP. (c) Conversion of nonpurified NCA in a conventional DCM solution under anhydrous condition and through biphasic SIMPLE strategy under open-air condition. Reproduced with permission from ref 38. Copyright 2019 National Academy of Sciences. (d) GPC traces of the obtained polypeptides from nonpurified monomers in the absence and presence of *n*-hexylamine as an amine scavenger (AS). (e) GPC traces of PEG-polypeptide from purified monomers on a small scale (10 mg monomer) and nonpurified monomers on a large scale (1 g starting amino acid). Reproduced with permission from ref 44. Copyright 2020 American Chemical Society.

block copolypeptides with desired block numbers, composition, block lengths, and block sequence were prepared within a few hours.[39] The fast polymerization kinetics of CCP guaranteed the minimal loss of propagating amines, which was critical to maintaining a high blocking efficiency and complete shift of polymer peaks on the gel permeation chromatography (GPC) traces. For instance, the synthesis of an icosablock copolypeptides was finished within 5 h with high monomer conversion and low dispersity ($Đ < 1.1$) (Figure 9d).

5.3. Direct Polymerization of Nonpurified Monomers

Besides the undesired side reactions, another issue that greatly limits the application of polypeptides is the laborious purification of NCA monomers. During the synthesis of NCA monomer, various acidic or electrophilic impurities were generated,[56] which would react with the propagating polypeptide chains, slowing down or even terminating the polymerization (Figure 10a). Repetitive recrystallization or flash column chromatography under strictly anhydrous conditions are therefore necessary to purify NCA monomers, which require sufficient expertise to minimize the impurities. As a result, a polymerization system devoid of monomer purification steps would not only lower the cost of polypeptide materials, but also allow the synthesis of polypeptides by nonexperts.

Because most impurities are either highly soluble in water (e.g., HCl) or tend to hydrolyze (e.g., phosgene), we reasoned that the biphasic CCP would be an ideal system to conduct direct polymerization of the nonpurified monomer. Indeed, HCl exhibited a large partition coefficient in water/DCM ($P = 79 \pm 10$),[38] with polymerization-essential components (i.e., NCA monomers and propagating polypeptide chains) remaining in the DCM phase. Combined with the fast biphasic CCP that minimized the water-induced NCA degradation (vide supra), we successfully carried out the controlled polymerization of nonpurified NCA monomers (Figure 10b).[38] In a typical procedure, the polymerization was able to finish within 20 min (Figure 10c). This polymerization strategy, termed as SIMPLE (Segregation-Induced Monomer-Purification and initiator-Localization promoted rate-Enhancement), circumvents the water-free setups and monomer purification procedures at the same time, thus significantly lowering the polymerization cost and shortening the synthetic procedure of polypeptides from days to hours. It has to be noted that the SIMPLE strategy is not limited to the biphasic CCP initiating system from interfacially anchored PEG-PBLG. Any water-compatible accelerated polymerization system can be incorporated into the biphasic design as long as the polymerization rate outpaces water-induced side reactions.[38]

Due to the complex composition of nonpurified NCAs, a water/oil phase segregation process may not effectively remove all impurities. The impurities with poor water-solubility will stay in the oil phase and terminate the propagating chains. Therefore, the initial SIMPLE design failed to polymerize some special nonpurified monomers, including oily monomers, monomers from amino acids with multistep synthesis, and monomers with high phosgene feeding (Figure 10d).[44] Liquid

https://doi.org/10.1021/accountsmr.3c00046
Acc. Mater. Res. 2023, 4, 604−615

chromatography−mass spectrometry analysis revealed that these batches of nonpurified NCA were rich in phosgene and its derivatives. To solve this issue, we adapted the SIMPLE method to the nonpurified NCA by adding a small-molecular amine scavenger,[44] which was not able to compete with biphasic CCP but effectively protected the propagating chains from the phosgene species (Figure 10d).

The SIMPLE strategy was successfully extended to various nonpurified NCA monomers,[38,44,47] including water-soluble γ-(2-(2-(2-methoxyethoxy)ethoxy)ethoxy)-esteryl-L-glutamate NCA (EG_3Glu-NCA),[47] albeit with a lower yield due to the partition of the monomer in the aqueous phase. With a simplified procedure compared with the conventional method, streamlined gram-scale synthesis of polypeptides from amino acids (i.e., NCA as an intermediate) was demonstrated within several hours.[44] The obtained polypeptides showed a similar GPC profile with those from sub-100 mg scale synthesis (Figure 10e), suggesting the potential of our strategy for commercial, large-scale production of polypeptide materials.

6. CONCLUSION AND PERSPECTIVE

The in-depth studies on the CCP offer new insights into biomimetic catalysis, which guides the design of catalytic systems by highlighting the importance of solvent environment and confined molecular interactions. Additionally, the development of various CCP systems facilitates the preparation of polypeptide materials, which is achieved by accelerating the main polymerization that minimizes side reactions. The restricted polymerization conditions as well as laborious purification steps are therefore circumvented, which significantly lowers the cost and reduce the technical constraints of polypeptide synthesis, making polypeptide materials accessible to nonexperts. Nevertheless, several questions remain to be answered in order to fully understand the CCP system. For instance, the detailed mechanism of proximity-induced rate acceleration is still not clear, which may involve complex interactions among multiple propagating polypeptides and monomers.[32,42] In addition, the two-stage kinetics of CCP intrinsically produces polypeptide materials with oligomeric species (i.e., propagating chains trapped in the first stage). Several CCP systems have to rely on the use of pre-existing α-helical macroinitiators to prepare polypeptide materials with predictable MWs, which obviously complicates the synthetic process.[38,46] Therefore, further optimization of polymerization conditions, including temperature, solvents, and the addition of catalysts/inhibitors, may help tune the coil-to-helix transition or minimize the rate differences between the random-coiled and α-helical polypeptides.

While the development of CCP enriches the toolbox of polypeptide synthesis, the advances in the polypeptide field also rely on downstream studies on the materials property and the application of polypeptide materials. For instance, CCP generates versatile polypeptide materials that are difficult to prepare with conventional methods, whose unique functions are yet to be demonstrated. Specifically, the branched polypeptides, which are easily synthesized with multi-amine CCP systems, may exhibit unique biomedical performance considering their spatially defined structures and the multivalency effect. Star- and brush-shaped polypeptides have already shown promising performance as drug carriers, antimicrobial agents, and therapeutics for autoimmune diseases. Additionally, the polypeptides with ultrahigh MWs may exhibit interesting mechanical properties that are not found in polypeptides with DP < 200. On the other hand, CCP may generate unique nanoassemblies in situ with the polymerization-induced self-assembly strategy considering the accelerated kinetics.[43,57,58] With adequate knowledge of the structure−property relationship of polypeptide materials, we believe that polypeptide materials will reveal their full potential, which may exhibit even superior properties compared with their natural protein analogues.

AUTHOR INFORMATION

Corresponding Authors

Yao Lin − *Department of Chemistry and Polymer Program, Institute of Materials Science, University of Connecticut, Storrs, Connecticut 06269, United States;* orcid.org/0000-0001-5227-2663; Email: yao.lin@uconn.edu

Jianjun Cheng − *Research Center for Industries of the Future and School of Engineering, Westlake University, Hangzhou 310030, China;* orcid.org/0000-0003-2561-9291; Email: chengjianjun@westlake.edu.cn

Ziyuan Song − *Institute of Functional Nano & Soft Materials (FUNSOM), Jiangsu Key Laboratory for Carbon-Based Functional Materials & Devices, Soochow University, Suzhou 215123, China;* orcid.org/0000-0002-3165-3712; Email: zysong@suda.edu.cn

Authors

Wanying Wang − *Institute of Functional Nano & Soft Materials (FUNSOM), Jiangsu Key Laboratory for Carbon-Based Functional Materials & Devices, Soochow University, Suzhou 215123, China*

Hailin Fu − *Department of Chemistry and Polymer Program, Institute of Materials Science, University of Connecticut, Storrs, Connecticut 06269, United States;* orcid.org/0000-0002-3972-7659

Complete contact information is available at: https://pubs.acs.org/10.1021/accountsmr.3c00046

Notes

The authors declare no competing financial interest.

Biographies

Wanying Wang is a Ph.D. candidate in Prof. Ziyuan Song's research group at the Institute of Functional Nano and Soft Materials (FUNSOM) at Soochow University. She received her B.S. degree in Materials Science and Engineering from Xiangtan University. Her research interest includes the design and synthesis of functional polypeptides for biomedical applications.

Hailin Fu is currently a postdoc in the Chemistry and Chemical Engineering department of Eindhoven University of Technology, NL. She obtained her B.S. degree from the Chemistry Department of Nanjing University and her Ph.D. degree from the Chemistry Department of University of Connecticut under the guidance of Prof. Yao Lin. After her Ph.D. work on the cooperative behaviors of complex macromolecules, she joined Prof. Ting Xu's lab as a postdoc at University of California, Berkeley and studied the impact of sequences on random copolymers. Her current work in Prof. E. W. Meijer's group is focused on supramolecular polymers.

Yao Lin is a Professor of the Chemistry and Polymer Program at the Institute of Materials Science at the University of Connecticut, Storrs. He obtained his B.S. degree in Macromolecular Science from Fudan University, and his Ph.D. degree in Polymer Science and Engineering

https://doi.org/10.1021/accountsmr.3c00046
Acc. Mater. Res. 2023, 4, 604−615

from the University of Massachusetts, Amherst. After completing his George W. Beadle postdoctoral fellowship at the Argonne National Laboratory and the University of Chicago in the fields of biosciences and chemistry, he joined the faculty at the University of Connecticut in late 2008. He took a sabbatical at the Institute of Complex Molecular Systems at the Eindhoven University of Technology in 2015 and 2021. His research focuses on applying the biological concepts to the synthetic and hybrid macromolecules, for development of new functional materials with cooperative behaviors.

Jianjun Cheng is a Chair Professor of Materials Science and Engineering and Dean of the School of Engineering at Westlake University. He obtained his B.S. degree in Chemistry from Nankai University, his M.S. degree in Chemistry from Southern Illinois University at Carbondale, and his Ph.D. degree in Materials Science from the University of California, Santa Barbara. He worked as a Senior Scientist at Insert Therapeutics, Inc. and did his postdoctoral research at MIT. Before joining Westlake University in 2021, he was on the faculty in the Department of Materials Science and Engineering at the University of Illinois at Urbana−Champaign between 2005 and 2021. His research interests include polypeptide biomaterials, nanomedicine, and cancer targeting.

Ziyuan Song is a Professor at the Institute of Functional Nano and Soft Materials (FUNSOM) at Soochow University. He obtained his B.S. degree in Materials Chemistry and Ph.D. degree in Materials Science and Engineering from Peking University and the University of Illinois at Urbana−Champaign, respectively, the latter under the guidance of Prof. Jianjun Cheng. After a postdoctoral position with Prof. Cheng, he joined Soochow University in 2021. His research interests include polymerization behavior, preparation strategy, and conformation studies of synthetic polypeptides for biomedical applications.

■ ACKNOWLEDGMENTS

This work is supported by the National Natural Science Foundation of China (22101194 for Z.S. and 52233015 for J.C.), the U.S. National Science Foundation (DMR-1809497 and DMR-2210590 for Y.L.), Natural Science Foundation of Jiangsu Province (BK20210733 for Z.S.), Suzhou Municipal Science and Technology Bureau (ZXL2021447 for Z.S.), Collaborative Innovation Center of Suzhou Nano Science & Technology, the 111 Project. Joint Suzhou Key Laboratory of Nanotechnology and Biomedicine, and Westlake Education Foundation.

■ REFERENCES

(1) Deming, T. J. Synthetic polypeptides for biomedical applications. *Prog. Polym. Sci.* **2007**, *32*, 858−875.
(2) Kataoka, K.; Harada, A.; Nagasaki, Y. Block copolymer micelles for drug delivery: design, characterization and biological significance. *Adv. Drug Delivery Rev.* **2012**, *64*, 37−48.
(3) He, C.; Zhuang, X.; Tang, Z.; Tian, H.; Chen, X. Stimuli-sensitive synthetic polypeptide-based materials for drug and gene delivery. *Adv. Healthc. Mater.* **2012**, *1*, 48−78.
(4) Deng, C.; Wu, J.; Cheng, R.; Meng, F.; Klok, H.-A.; Zhong, Z. Functional polypeptide and hybrid materials: precision synthesis via α-amino acid *N*-carboxyanhydride polymerization and emerging biomedical applications. *Prog. Polym. Sci.* **2014**, *39*, 330−364.
(5) Song, Z.; Han, Z.; Lv, S.; Chen, C.; Chen, L.; Yin, L.; Cheng, J. Synthetic polypeptides: from polymer design to supramolecular assembly and biomedical application. *Chem. Soc. Rev.* **2017**, *46*, 6570−6599.
(6) Rasines Mazo, A.; Allison-Logan, S.; Karimi, F.; Chan, N. J.-A.; Qiu, W.; Duan, W.; O'Brien-Simpson, N. M.; Qiao, G. G. Ring opening polymerization of α-amino acids: advances in synthesis, architecture and applications of polypeptides and their hybrids. *Chem. Soc. Rev.* **2020**, *49*, 4737−4834.
(7) Carlsen, A.; Lecommandoux, S. Self-assembly of polypeptide-based block copolymer amphiphiles. *Curr. Opin. Colloid Interface Sci.* **2009**, *14*, 329−339.
(8) Lu, H.; Wang, J.; Song, Z.; Yin, L.; Zhang, Y.; Tang, H.; Tu, C.; Lin, Y.; Cheng, J. Recent advances in amino acid *N*-carboxyanhydrides and synthetic polypeptides: chemistry, self-assembly and biological applications. *Chem. Commun.* **2014**, *50*, 139−155.
(9) Shen, Y.; Fu, X.; Fu, W.; Li, Z. Biodegradable stimuli-responsive polypeptide materials prepared by ring opening polymerization. *Chem. Soc. Rev.* **2015**, *44*, 612−622.
(10) Deming, T. J. Synthesis of side-chain modified polypeptides. *Chem. Rev.* **2016**, *116*, 786−808.
(11) Melnyk, T.; Đorđević, S.; Conejos-Sánchez, I.; Vicent, M. J. Therapeutic potential of polypeptide-based conjugates: rational design and analytical tools that can boost clinical translation. *Adv. Drug Delivery Rev.* **2020**, *160*, 136−169.
(12) Deng, C.; Zhang, Q.; Guo, J.; Zhao, X.; Zhong, Z. Robust and smart polypeptide-based nanomedicines for targeted tumor therapy. *Adv. Drug Delivery Rev.* **2020**, *160*, 199−211.
(13) Zhang, Y.; He, P.; Zhang, P.; Yi, X.; Xiao, C.; Chen, X. Polypeptides-drug conjugates for anticancer therapy. *Adv. Healthc. Mater.* **2021**, *10*, 2001974.
(14) Liu, Y.; Yin, L. α-Amino acid *N*-carboxyanhydride (NCA)-derived synthetic polypeptides for nucleic acids delivery. *Adv. Drug Delivery Rev.* **2021**, *171*, 139−163.
(15) Song, Z.; Fu, H.; Wang, R.; Pacheco, L. A.; Wang, X.; Lin, Y.; Cheng, J. Secondary structures in synthetic polypeptides from *N*-carboxyanhydrides: design, modulation, association, and material applications. *Chem. Soc. Rev.* **2018**, *47*, 7401−7425.
(16) Bonduelle, C. Secondary structures of synthetic polypeptide polymers. *Polym. Chem.* **2018**, *9*, 1517−1529.
(17) van Hest, J. C. M.; Tirrell, D. A. Protein-based materials, toward a new level of structural control. *Chem. Commun.* **2001**, 1897−1904.
(18) Merrifield, R. B. Solid phase peptide synthesis. I. The synthesis of a tetrapeptide. *J. Am. Chem. Soc.* **1963**, *85*, 2149−2154.
(19) Kricheldorf, H. R. Polypeptides and 100 years of chemistry of α-amino acid *N*-carboxyanhydrides. *Angew. Chem., Int. Ed.* **2006**, *45*, 5752−5784.
(20) Leuchs, H. Ueber die glycin-carbonsäure. *Ber. Dtsch. Chem. Ges.* **1906**, *39*, 857−861.
(21) Blout, E. R.; Idelson, M. Polypeptides. IX. The kinetics of strong-base initiated polymerizations of amino acid-*N*-carboxyanhydrides. *J. Am. Chem. Soc.* **1956**, *78*, 3857−3858.
(22) Idelson, M.; Blout, E. R. Polypeptides. XV. Infrared spectroscopy and the kinetics of the synthesis of polypeptides: primary amine initiated reactions. *J. Am. Chem. Soc.* **1957**, *79*, 3948−3955.
(23) Deming, T. J. Facile synthesis of block copolypeptides of defined architecture. *Nature* **1997**, *390*, 386−389.
(24) Dimitrov, I.; Schlaad, H. Synthesis of nearly monodisperse polystyrene-polypeptide block copolymers via polymerisation of *N*-carboxyanhydrides. *Chem. Commun.* **2003**, 2944−2945.
(25) Aliferis, T.; Iatrou, H.; Hadjichristidis, N. Living polypeptides. *Biomacromolecules* **2004**, *5*, 1653−1656.
(26) Lu, H.; Cheng, J. Hexamethyldisilazane-mediated controlled polymerization of α-amino acid *N*-carboxyanhydrides. *J. Am. Chem. Soc.* **2007**, *129*, 14114−14115.
(27) Habraken, G. J. M.; Peeters, M.; Dietz, C. H. J. T.; Koning, C. E.; Heise, A. How controlled and versatile is *N*-carboxy anhydride (NCA) polymerization at 0 °C? Effect of temperature on homo-, block- and graft (co)polymerization. *Polym. Chem.* **2010**, *1*, 514−524.
(28) Hadjichristidis, N.; Iatrou, H.; Pitsikalis, M.; Sakellariou, G. Synthesis of well-defined polypeptide-based materials via the ring-opening polymerization of α-amino acid *N*-carboxyanhydrides. *Chem. Rev.* **2009**, *109*, 5528−5578.

https://doi.org/10.1021/accountsmr.3c00046
Acc. Mater. Res. 2023, 4, 604−615

(29) Li, L.; Cen, J.; Pan, W.; Zhang, Y.; Leng, X.; Tan, Z.; Yin, H.; Liu, S. Synthesis of polypeptides with high-fidelity terminal functionalities under NCA monomer-starved conditions. *Research* **2021**, *2021*, 9826046.
(30) Zou, J.; Fan, J.; He, X.; Zhang, S.; Wang, H.; Wooley, K. L. A facile glovebox-free strategy to significantly accelerate the syntheses of well-defined polypeptides by *N*-carboxyanhydride (NCA) ring-opening polymerizations. *Macromolecules* **2013**, *46*, 4223−4226.
(31) Zhao, W.; Gnanou, Y.; Hadjichristidis, N. From competition to cooperation: a highly efficient strategy towards well-defined (co)-polypeptides. *Chem. Commun.* **2015**, *51*, 3663−3666.
(32) Baumgartner, R.; Fu, H.; Song, Z.; Lin, Y.; Cheng, J. Cooperative polymerization of α-helices induced by macromolecular architecture. *Nat. Chem.* **2017**, *9*, 614−622.
(33) Wu, Y.; Zhang, D.; Ma, P.; Zhou, R.; Hua, L.; Liu, R. Lithium hexamethyldisilazide initiated superfast ring opening polymerization of alpha-amino acid *N*-carboxyanhydrides. *Nat. Commun.* **2018**, *9*, 5297.
(34) Yuan, J.; Zhang, Y.; Li, Z.; Wang, Y.; Lu, H. A S-Sn lewis pair-mediated ring-opening polymerization of α-amino acid *N*-carboxyanhydrides: fast kinetics, high molecular weight, and facile bioconjugation. *ACS Macro Lett.* **2018**, *7*, 892−897.
(35) Zhang, Y.; Liu, R.; Jin, H.; Song, W.; Augustine, R.; Kim, I. Straightforward access to linear and cyclic polypeptides. *Commun. Chem.* **2018**, *1*, 40.
(36) Zhao, W.; Lv, Y.; Li, J.; Feng, Z.; Ni, Y.; Hadjichristidis, N. Fast and selective organocatalytic ring-opening polymerization by fluorinated alcohol without a cocatalyst. *Nat. Commun.* **2019**, *10*, 3590.
(37) Chen, C.; Fu, H.; Baumgartner, R.; Song, Z.; Lin, Y.; Cheng, J. Proximity-induced cooperative polymerization in "hinged" helical polypeptides. *J. Am. Chem. Soc.* **2019**, *141*, 8680−8683.
(38) Song, Z.; Fu, H.; Wang, J.; Hui, J.; Xue, T.; Pacheco, L. A.; Yan, H.; Baumgartner, R.; Wang, Z.; Xia, Y.; Wang, X.; Yin, L.; Chen, C.; Rodríguez-López, J.; Ferguson, A. L.; Lin, Y.; Cheng, J. Synthesis of polypeptides via bioinspired polymerization of in situ purified *N*-carboxyanhydrides. *Proc. Natl. Acad. Sci. U. S. A.* **2019**, *116*, 10658−10663.
(39) Wang, X.; Song, Z.; Tan, Z.; Zhu, L.; Xue, T.; Lv, S.; Fu, Z.; Zheng, X.; Ren, J.; Cheng, J. Facile synthesis of helical multiblock copolypeptides: minimal side reactions with accelerated polymerization of *N*-carboxyanhydrides. *ACS Macro Lett.* **2019**, *8*, 1517−1521.
(40) Song, Z.; Fu, H.; Baumgartner, R.; Zhu, L.; Shih, K.-C.; Xia, Y.; Zheng, X.; Yin, L.; Chipot, C.; Lin, Y.; Cheng, J. Enzyme-mimetic self-catalyzed polymerization of polypeptide helices. *Nat. Commun.* **2019**, *10*, 5470.
(41) Jacobs, J.; Pavlović, D.; Prydderch, H.; Moradi, M.-A.; Ibarboure, E.; Heuts, J. P. A.; Lecommandoux, S.; Heise, A. Polypeptide nanoparticles obtained from emulsion polymerization of amino acid *N*-carboxyanhydrides. *J. Am. Chem. Soc.* **2019**, *141*, 12522−12526.
(42) Lv, S.; Kim, H.; Song, Z.; Feng, L.; Yang, Y.; Baumgartner, R.; Tseng, K.-Y.; Dillon, S. J.; Leal, C.; Yin, L.; Cheng, J. Unimolecular polypeptide micelles via ultrafast polymerization of *N*-carboxyanhydrides. *J. Am. Chem. Soc.* **2020**, *142*, 8570−8574.
(43) Grazon, C.; Salas-Ambrosio, P.; Ibarboure, E.; Buol, A.; Garanger, E.; Grinstaff, M. W.; Lecommandoux, S.; Bonduelle, C. Aqueous ring-opening polymerization-induced self-assembly (ROPISA) of *N*-carboxyanhydrides. *Angew. Chem., Int. Ed.* **2020**, *59*, 622−626.
(44) Xue, T.; Song, Z.; Wang, Y.; Zhu, B.; Zhao, Z.; Tan, Z.; Wang, X.; Xia, Y.; Cheng, J. Streamlined synthesis of PEG-polypeptides directly from amino acids. *Macromolecules* **2020**, *53*, 6589−6597.
(45) Wu, Y.; Chen, K.; Wu, X.; Liu, L.; Zhang, W.; Ding, Y.; Liu, S.; Zhou, M.; Shao, N.; Ji, Z.; Chen, J.; Zhu, M.; Liu, R. Superfast and water-insensitive polymerization on α-amino acid *N*-carboxyanhydrides to prepare polypeptides using tetraalkylammonium carboxylate as the initiator. *Angew. Chem., Int. Ed.* **2021**, *60*, 26063−26071.
(46) Xia, Y.; Song, Z.; Tan, Z.; Xue, T.; Wei, S.; Zhu, L.; Yang, Y.; Fu, H.; Jiang, Y.; Lin, Y.; Lu, Y.; Ferguson, A. L.; Cheng, J. Accelerated polymerization of *N*-carboxyanhydrides catalyzed by crown ether. *Nat. Commun.* **2021**, *12*, 732.
(47) Tan, Z.; Song, Z.; Xue, T.; Zheng, L.; Jiang, L.; Jiang, Y.; Fu, Z.; Nguyen, A.; Leal, C.; Cheng, J. Open-air synthesis of oligo(ethylene glycol)-functionalized polypeptides from non-purified *N*-carboxyanhydrides. *Biomater. Sci.* **2021**, *9*, 4120−4126.
(48) Hu, Y.; Tian, Z.-Y.; Xiong, W.; Wang, D.; Zhao, R.; Xie, Y.; Song, Y.-Q.; Zhu, J.; Lu, H. Water-assisted and protein-initiated fast and controlled ring-opening polymerization of proline *N*-carboxyanhydride. *Natl. Sci. Rev.* **2022**, *9*, nwac033.
(49) Yang, F.; Liu, Z.; Si, W.; Song, Z.; Yin, L.; Tang, H. Facile preparation of polysaccharide-polypeptide conjugates via a biphasic solution ring-opening polymerization. *ACS Macro Lett.* **2022**, *11*, 663−668.
(50) Fu, H.; Baumgartner, R.; Song, Z.; Chen, C.; Cheng, J.; Lin, Y. Generalized model of cooperative covalent polymerization: connecting the supramolecular binding interactions with the catalytic behavior. *Macromolecules* **2022**, *55*, 2041−2050.
(51) Oosawa, F.; Kasai, M. A theory of linear and helical aggregations of macromolecules. *J. Mol. Biol.* **1962**, *4*, 10−21.
(52) Oosawa, F.; Asakura, S. *Thermodynamics of the polymerization of protein*; Academic Press: New York, 1975.
(53) De Greef, T. F. A.; Smulders, M. M. J.; Wolffs, M.; Schenning, A. P. H. J.; Sijbesma, R. P.; Meijer, E. W. Supramolecular polymerization. *Chem. Rev.* **2009**, *109*, 5687−5754.
(54) Zhao, D.; Moore, J. S. Nucleation-elongation: a mechanism for cooperative supramolecular polymerization. *Org. Biomol. Chem.* **2003**, *1*, 3471−3491.
(55) Sela, M.; Berger, A. The mechanism of polymerization of *N*-carboxy-α-amino acid anhydrides. *J. Am. Chem. Soc.* **1953**, *75*, 6350−6351.
(56) Katchalski, E.; Sela, M. Synthesis and chemical properties of poly-α-amino acids. In *Advances in Protein Chemistry*; Anfinsen, C. B., Anson, M. L., Bailey, K., Edsall, J. T., Eds.; Academic Press, 1958; Vol. *13*, pp 243−492.
(57) Jiang, J.; Zhang, X.; Fan, Z.; Du, J. Ring-opening polymerization of *N*-carboxyanhydride-induced self-assembly for fabricating biodegradable polymer vesicles. *ACS Macro Lett.* **2019**, *8*, 1216−1221.
(58) Li, H.; Cornel, E. J.; Fan, Z.; Du, J. Chirality-controlled polymerization-induced self-assembly. *Chem. Sci.* **2022**, *13*, 14179−14190.

https://doi.org/10.1021/accountsmr.3c00046
Acc. Mater. Res. 2023, 4, 604−615